Synthesis of hydroxylated group IV metal oxides inside *hollow* graphitised carbon nanofibres: nano-sponges and nanoreactors for enhanced decontamination of organophosphates.

Maxwell A. Astle,[a] Graham A. Rance,[a,b] Michael W. Fay,[b] Stuart Notman,[c] Mark R. Sambrook,[c] and Andrei N. Khlobystov*[,a,b].

[a.] *School of Chemistry, University of Nottingham, University Park, NG7 2RD, UK.*
[b.] *Nanoscale and Microscale Research Centre, University of Nottingham, University Park, NG7 2RD, UK.*
[c.] *CBR Division, Defence Science and Technology Laboratory (Dstl), Porton Down, Salisbury, Wiltshire, SP4 0JQ, UK.*

Supporting Information

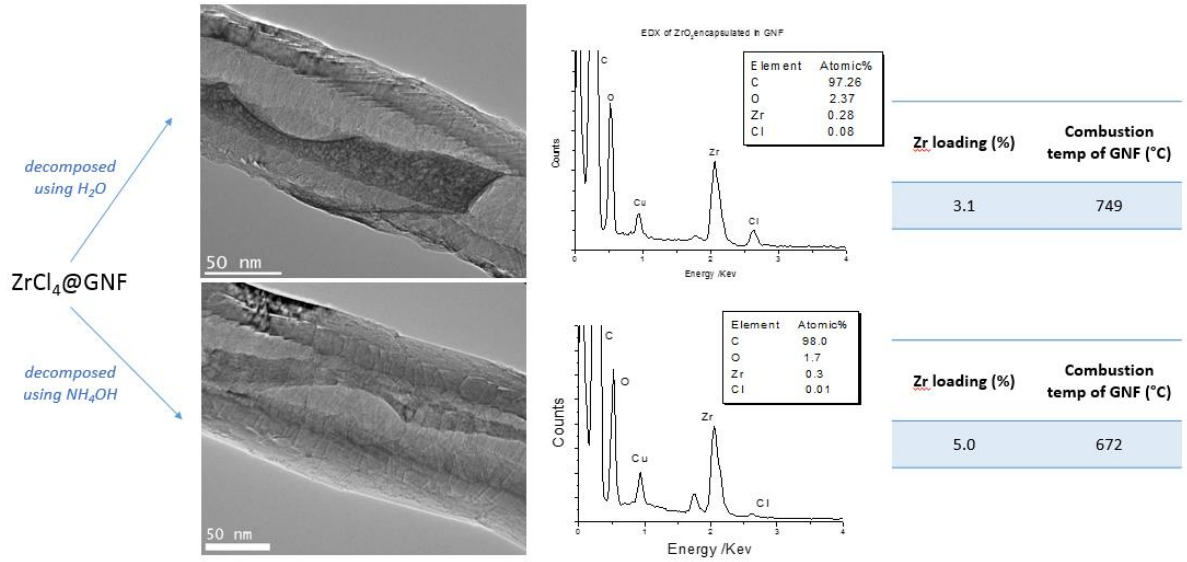

Zr loading (%)	Combustion temp of GNF (°C)
3.1	749

Zr loading (%)	Combustion temp of GNF (°C)
5.0	672

Figure S1 – Comparative $ZrCl_4$ hydrolysis with water or ammonium hydroxide. TGA indicates that a higher loading is obtained when ammonium hydroxide is used due to the formation of less water-soluble species. An increased electronic interaction between the GNF and the intercalant evidenced by a decrease in the combustion temperature supports the formation of a composite nanostructure with more Lewis acidic properties. EDX spectroscopy shows a higher residual chloride quantity for the water hydrolysed system indicating less complete hydrolysis when compared to the ammonium hydroxide route. TEM does appear to show similar encapsulated species, however, lower loadings can be confirmed using this technique also.

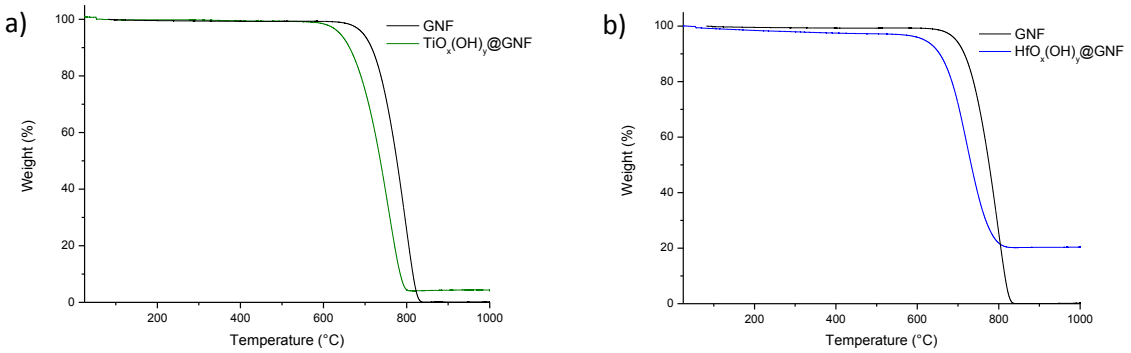

Figure S2 – Thermogravimetric analysis of a) $TiO_x(OH)_y$@GNF and b) $HfO_x(OH)_y$@GNF composite materials. Residual weights of 3% and 20%, respectively, were observed. Both thermograms show a downshift of the GNF combustion temperature (ΔT_{ox} = 40 and 76 °C for Ti and Hf, respectively), indicative of electronic interactions between the carbon nanostructure and the intercalant, though these are not as significant as the zirconia analogue (ΔT_{ox} = 124 °C).

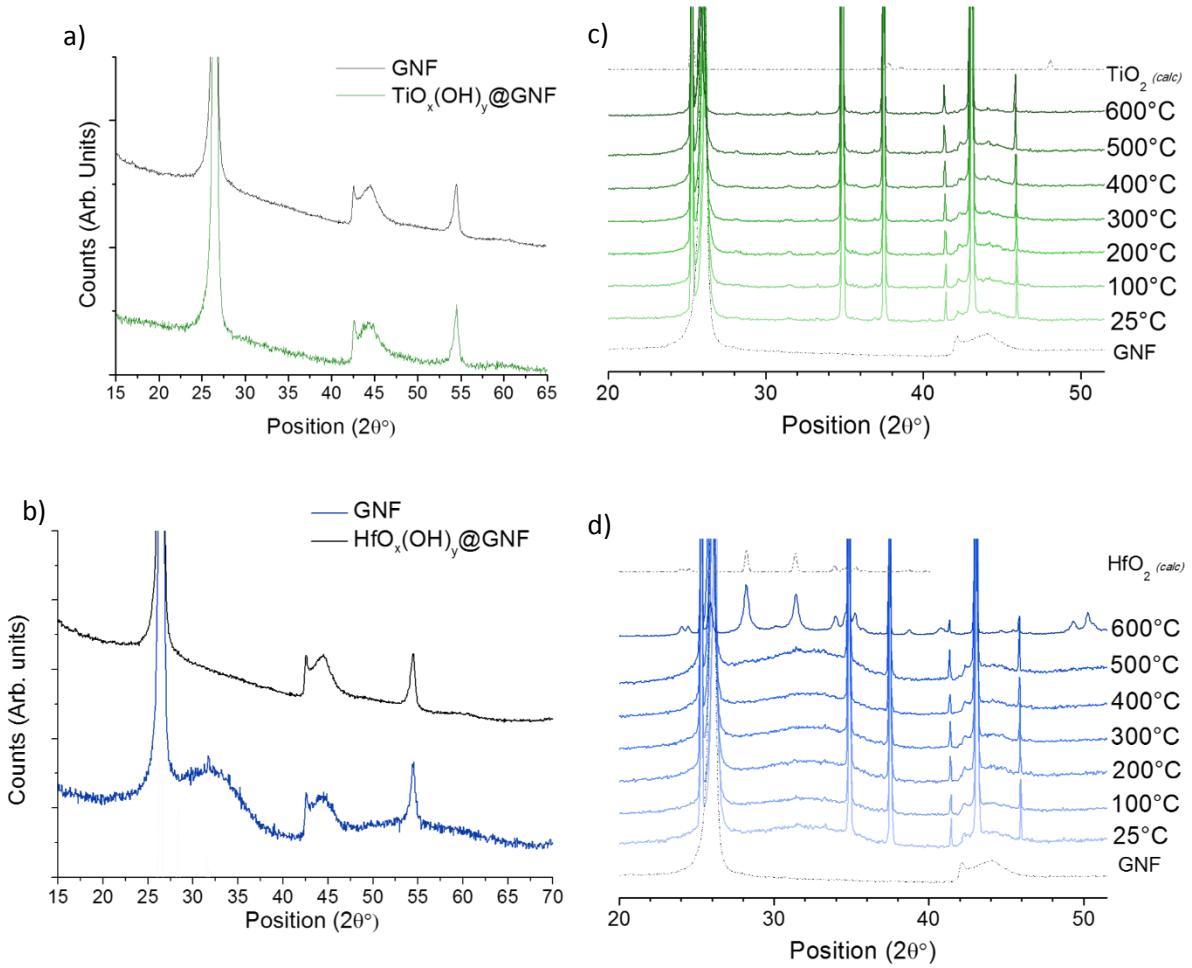

Figure S3 – PXRD analysis for a) $TiO_x(OH)_y$@GNF and b) $HfO_x(OH)_y$@GNF at room temperature, indicating the amorphous nature of the metal oxide formed. PXRD analysis for c) $TiO_x(OH)_y$@GNF and d) $HfO_x(OH)_y$@GNF samples heated to 600°C in air. Though difficult to confirm the formation of TiO_2 at 600 °C, owing to strong overlap with peaks from the alumina sample holder (2ϑ = 25.2, 34.7, 37.5, 41.3, 43.1 and 45.8°), the existence of HfO_2 at temperatures above 550 °C is clear (2ϑ =28.1 and 31.4°).

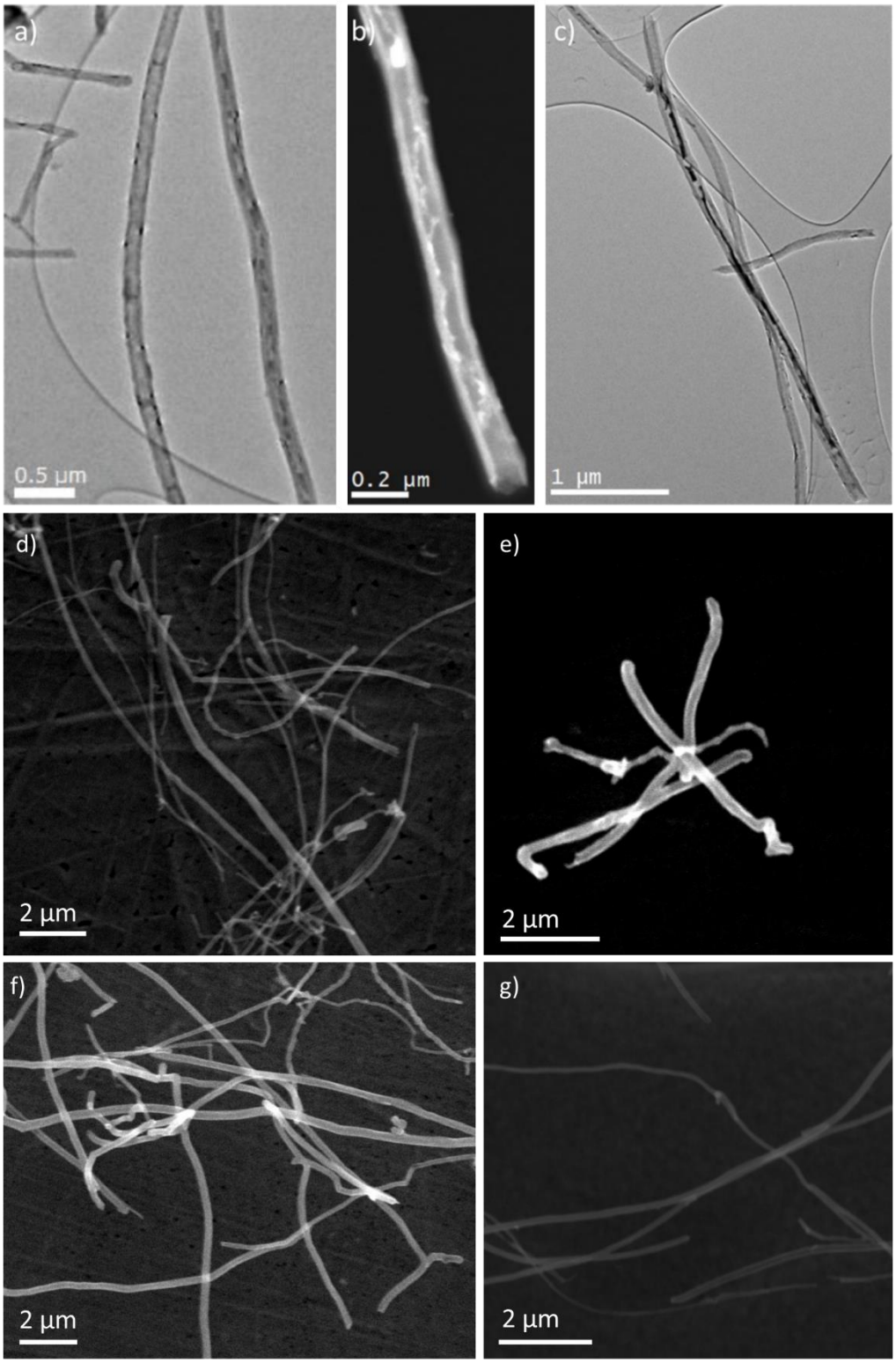

Figure S4 – Microstructural analysis of the $MO_x(OH)_y$ composite materials. Low magnification TEM of a) $TiO_x(OH)_y$@GNF, c) $HfO_x(OH)_y$@GNF and b) STEM of $ZrO_x(OH)_y$@GNF composite materials. SEM of d) empty GNF, e) $TiO_x(OH)_y$@GNF, f) $ZrO_x(OH)_y$@GNF and g) $HfO_x(OH)_y$@GNF.

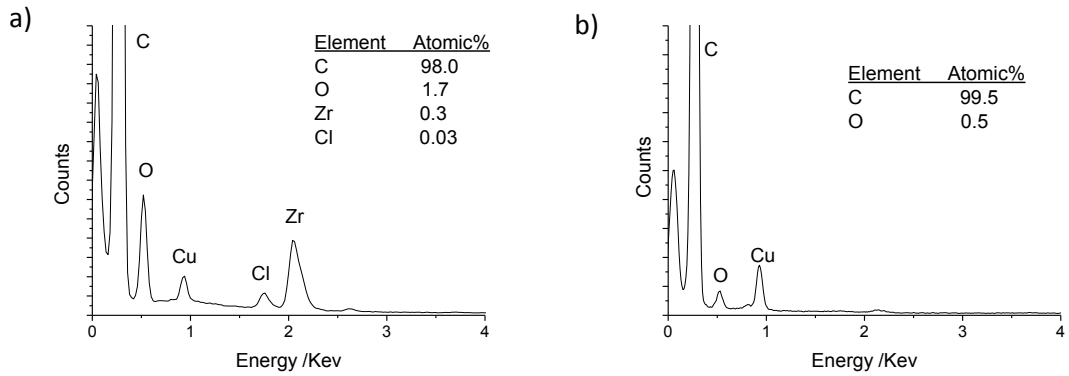

Figure S5 – Representative EDX spectra of GNF with (a) and without (b) group IV metal oxyhydroxide encapsulated species. The ratio of atomic percentages of oxygen and chlorine to the metal were measured and calculated using EDX spectroscopy. The metal coordination number was estimated from atomic percentages of chloride and oxygen.

Table S1 – The percentage weight loading of composite materials calculated from thermogravimetric analysis and atomic percentage ratio of oxygen and chlorine to the metal measured and calculated using EDX spectroscopy. Kα values used for carbon, oxygen chlorine and titanium, Lα value used for zirconium and Mα values used for hafnium. The metal coordination number estimated from atomic percentages of chloride and oxygen containing group, which are likely to surround the metal centre.

Material	Weight % of metal oxide	M:O atomic % ratio	M:Cl atomic % ratio	M coordination number
$TiO_x(OH)_y$@GNF	7.9	(1:)3.5	(1:)0.3	3.8
$ZrO_x(OH)_y$@GNF	8.1	3.4	0.1	3.5
$HfO_x(OH)_y$@GNF	21.1	2.5	0.2	2.7

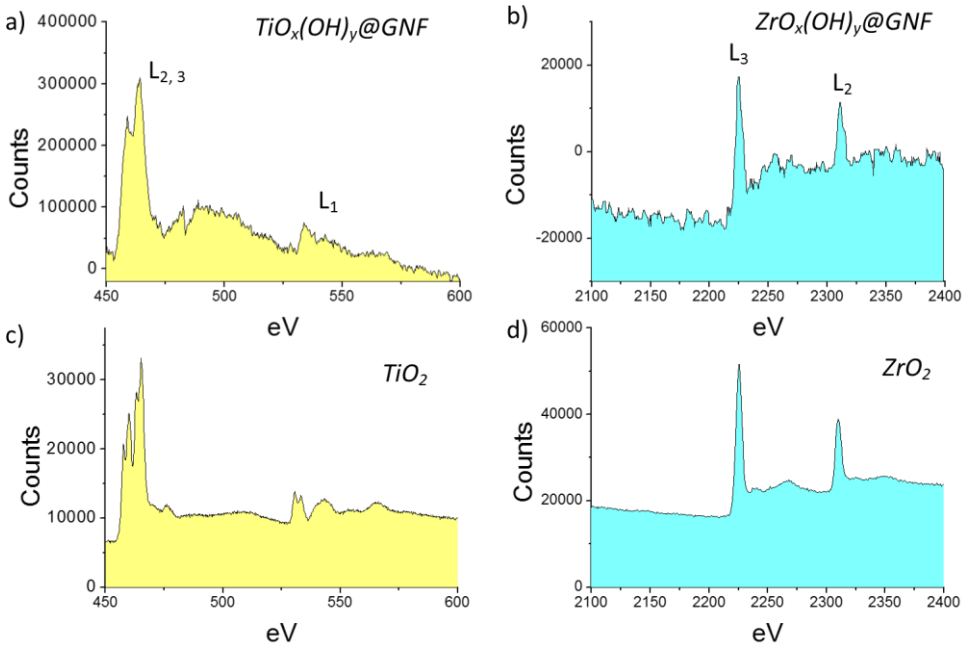

Figure S6 – Electron energy loss spectroscopy (EELS) analysis for a) $TiO_x(OH)_y$@GNF and b) $ZrO_x(OH)_y$@GNF. Reference EELS spectra of c) Ti and d) Zr as TiO_2 and ZrO_2, respectively, in the +4 oxidation state.[41] The Ti $L_{2,3}$ near edge structures at 459 and 465 eV match that for Ti^{4+} as lower oxidation states would be expected to shift slightly towards lower energy loss. Zr $L_{2,3}$ edge positions at 2225 and 2309 eV respectively also match Zr^{4+}. The Hf edge expected around 1800 eV proved too difficult to resolve due to low signal and overlap with the Si edge from the TEM grid.

Table S2 – BET surface analysis.

Sample	Metal oxide weight in sample (mg)	Surface area (m^2/g)	Pore Vol (cm/g)
GNF	0	22.30	0.0749
$Zr(OH)_4$ bulk	30.5	31.82	0.0704
$ZrO(OH)_2$@GNF	2.90	36.09	0.0826

Estimated surface area of encapsulated $ZrO(OH)_2$ = 141.25 m^2/g

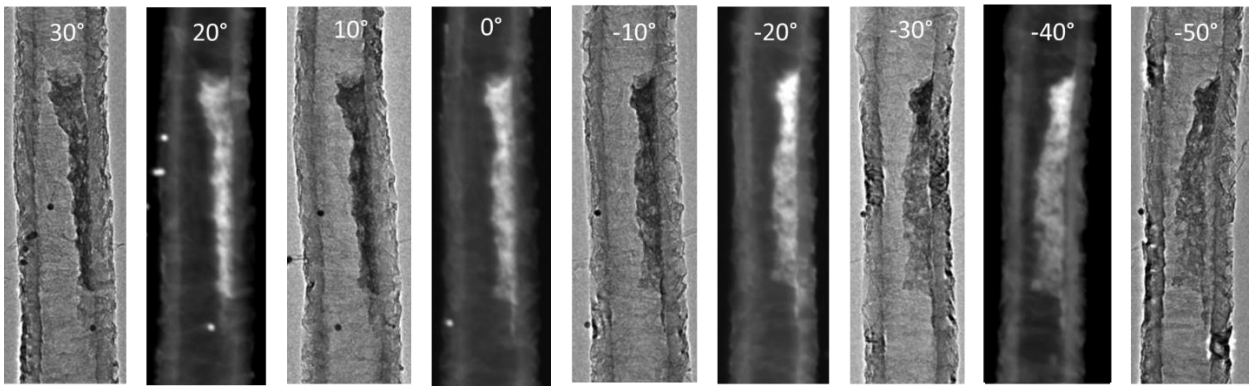

Figure S7 – Tomography using bright field TEM (for resolution) and dark field STEM images (for contrast) of $ZrO_x(OH)_y$@GNF. Au fiducial markers used to track tomography and aid reconstruction of the encapsulated species.

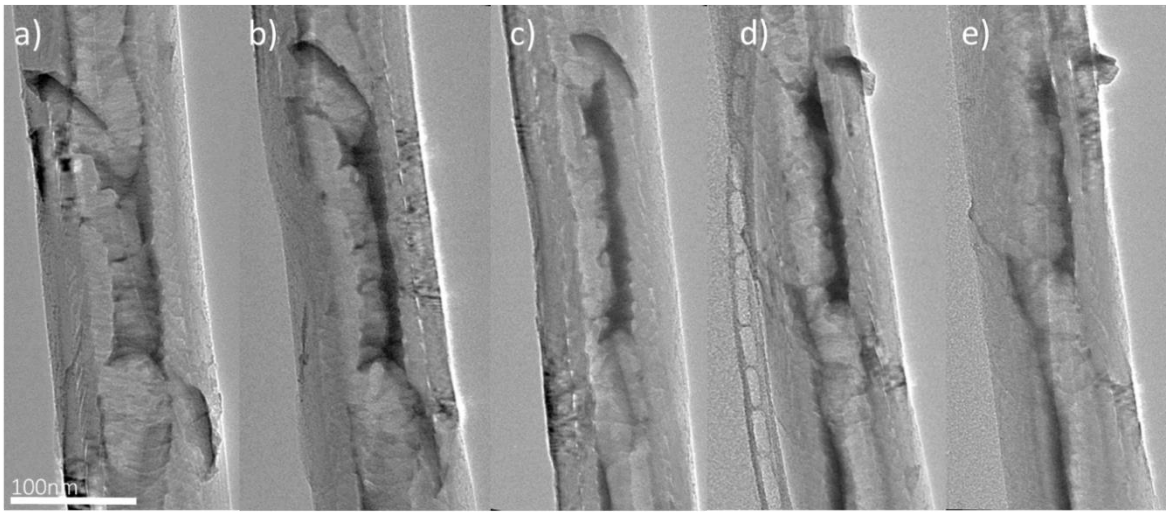

Figure S8 – *Tomography using bright field TEM of $HfO_x(OH)_y$@GNF species around GNF growth axis. a) 45°, b) 15°, c) -15°, d) -45° and e) -55°.*

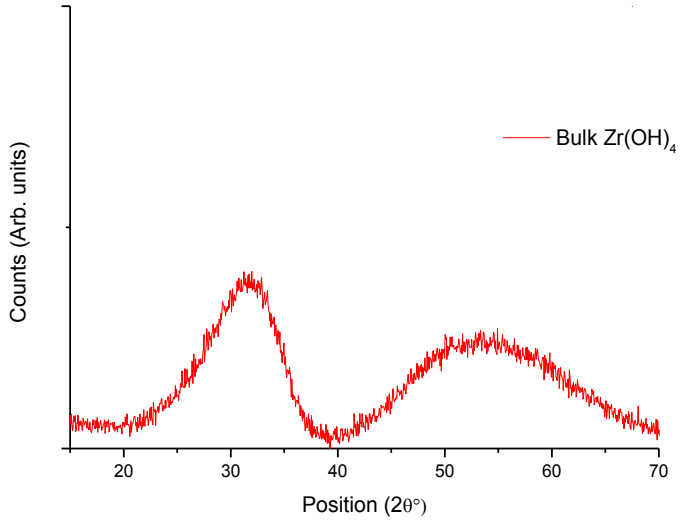

Figure S9 – PXRD analysis of bulk zirconia hydroxide. Broad peaks at 2ϑ= 30° confirm the formation of $Zr(OH)_4$.[8]

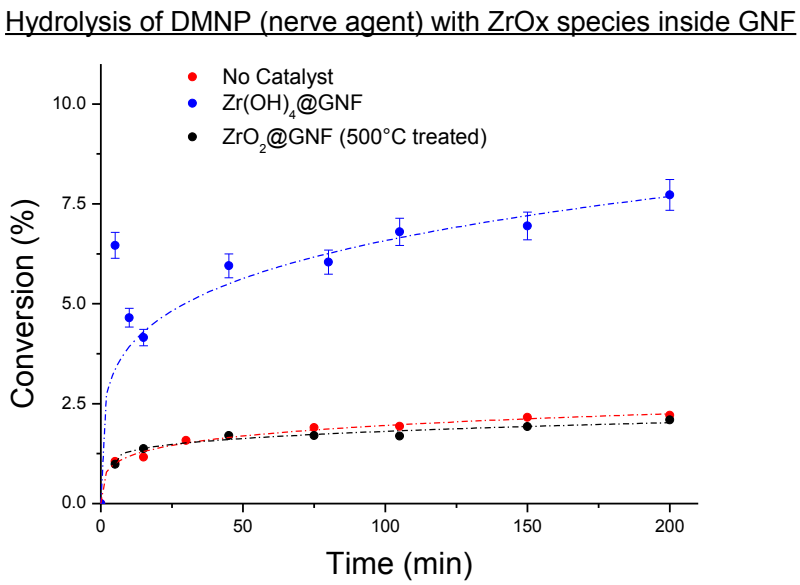

Figure S10 – Comparison of the DMNP hydrolysis using thermally annealed ZrO_2@GNF (black) and $ZrO(OH)_2$@GNF (blue). A significant difference in DMNP conversion is attributed to the loss of bridging hydroxyl groups and Lewis acidity of the nanocatalyst upon thermal treatment, which are key for the hydrolysis reaction.

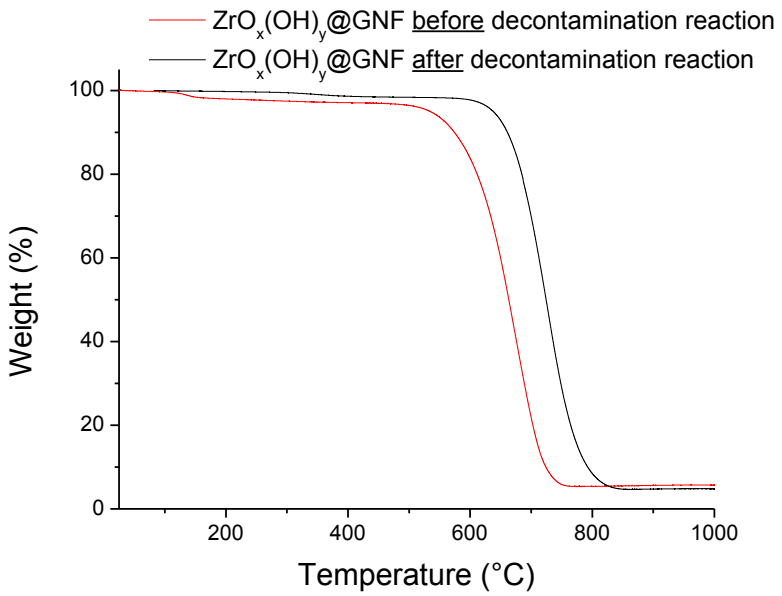

Figure S11 – TGA profile of $ZrO_x(OH)_y$@GNF catalyst before and after the DMNP hydrolysis reaction. Minimal change to the loading of catalyst was observed; however, an increase in the combustion temperature of GNF was noted, indicating lower Lewis acidity after the decontamination reaction. The weight loss below 150℃, which is related to the loss of hydroxyl groups on the surface, is also not present after the hydrolysis reaction.

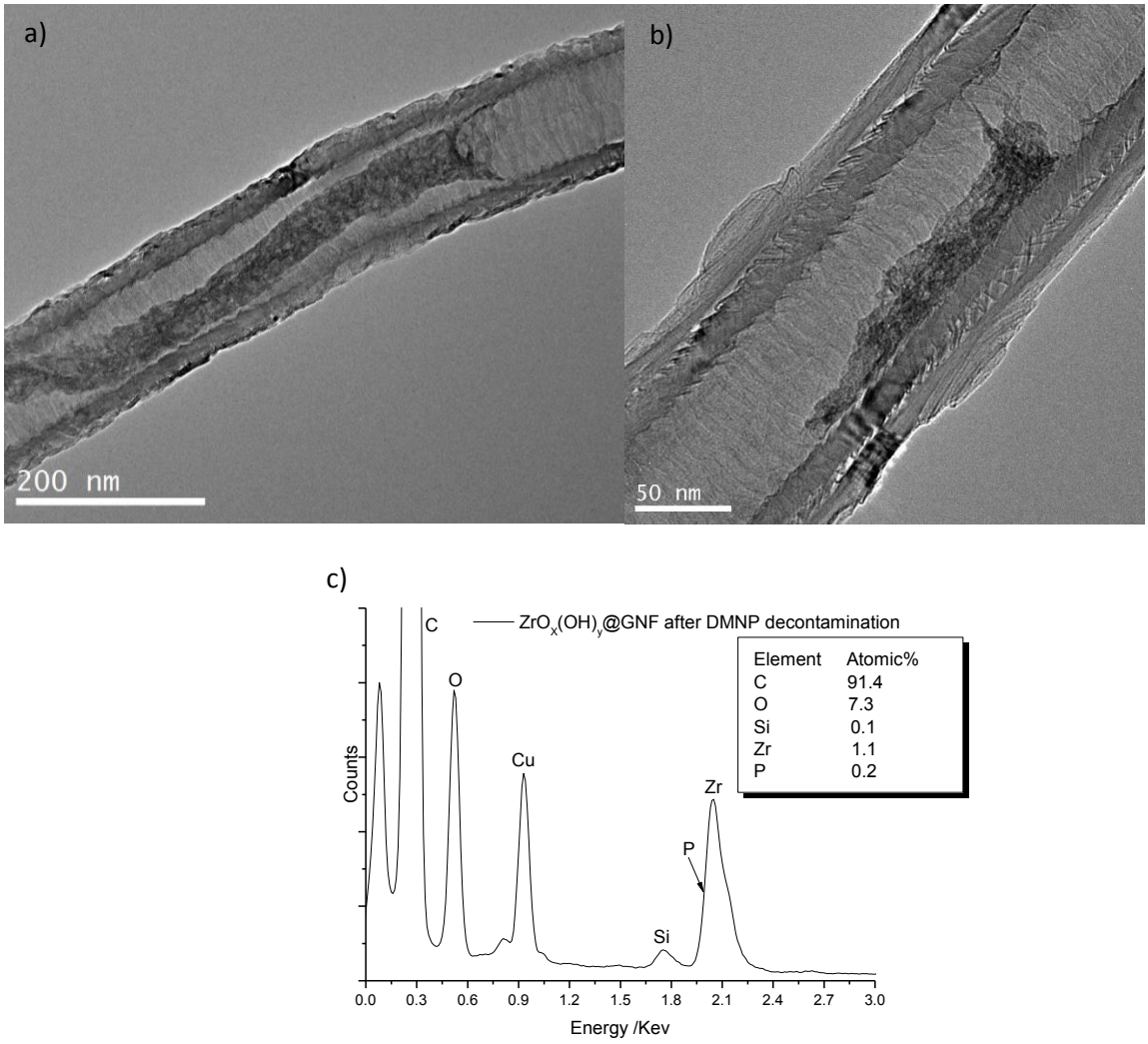

Figure S12 – a-b) TEM and c) EDX analysis of $ZrO_x(OH)_y$@GNF after the DMNP hydrolysis reaction, indicating the retention of the nanocatalyst within the internal channel of GNF. Instrument software indicates the presence of phosphorus, supporting the poisoning of the catalyst.